Pattern of charge ordering in quasi-one-dimensional organic charge-transfer solids

R. T. Clay,[1,2,*] S. Mazumdar,[1] and D. K. Campbell[3]
[1]*Department of Physics, University of Arizona, Tucson, Arizona 85721*
[2]*Cooperative Excitation Project ERATO, Japan Science and Technology Corporation (JST), Tucson, Arizona 85721*
[3]*Departments of Electrical and Computer Engineering and Physics, Boston University, Boston, Massachusetts 02215*
(Received 22 October 2002; published 21 March 2003)

We examine two recently proposed models of charge ordering (CO) in the nominally $\frac{1}{4}$-filled, quasi-one-dimensional (1D) organic charge-transfer solids (CTS). The two models are characterized by site charge density "cartoons" $\ldots 1010 \ldots$ and $\ldots 1100 \ldots$, respectively. We use the Peierls-extended Hubbard model to incorporate both electron-electron (e-e) and electron-phonon (e-ph) interactions. We first compare the results, for the purely electronic Hamiltonian, of exact many-body calculations with those of Hartree-Fock (HF) mean-field theory. We find that HF gives qualitatively and quantitatively incorrect values for the critical nearest-neighbor Coulomb repulsion (V_c) necessary for $\ldots 1010 \ldots$ order to become the ground state. Second, we establish that spin-Peierls order can occur in either the $\ldots 1100 \ldots$ and $\ldots 1010 \ldots$ states and calculate the phase diagram including both on-site and intrasite e-ph interactions. Third, we discuss the expected temperature dependence of the CO and metal-insulator transitions for both $\ldots 1010 \ldots$ and $\ldots 1100 \ldots$ CO states. Finally, we show that experimental observations clearly indicate the $\ldots 1100 \ldots$ CO in the 1:2 anionic CTS and the $(TMTSF)_2X$ materials, while the results for $(TMTTF)_2X$ with narrower one-electron bandwidths are more ambiguous, likely because the nearest-neighbor Coulomb interaction in these materials is near V_c.

DOI: 10.1103/PhysRevB.67.115121 PACS number(s): 71.30.+h, 71.45.Lr, 75.30.Fv, 74.70.Kn

I. INTRODUCTION

Recent experiments[1–16] showing clear evidence for the existence of charge order (CO) in several 2:1 cationic organic charge-transfer solids (CTS) have stimulated considerable theoretical interest.[17–26] As these materials are nominally $\frac{1}{4}$-filled (one electron or hole per two sites) and involve electron-electron (e-e) interactions (including nearest-neighbor Coulomb repulsion V), the apparently obvious charge ordering in the quasi-1D (one-dimensional) CTS systems is the Wigner crystallike "$\ldots 1010 \ldots$" state, and numerous theoretical[20,26] and experimental[5,12–16] studies have argued for this possibility. The site occupancies "1" and "0" actually correspond to $0.5+\epsilon$ and $0.5-\epsilon$, respectively, with being ϵ an important measurable quantity. The $\ldots 1010 \ldots$ CO corresponds to a $4k_F$ CDW (charge-density wave) (spatial period 2), where $k_F=\pi/2a$ is the Fermi wave vector in the absence of Coulomb interactions, with a being the lattice constant. On the other hand, in previous work we[17–19] and others[22–25] have shown that for realistic values of V and when electron-phonon (e-ph) interactions are included, a "$\ldots 1100 \ldots$" charge ordering can become the ground state, and, importantly, that this CO state can explain the "mysterious" states observed in several CTS,[1–3] in which coexisting charge and spin-density waves *of the same periodicity* occur. The $\ldots 1100 \ldots$ CO corresponds to a $2k_F$ CDW (spatial period 4) and has a cooperative coexistence with the $2k_F$ bond-order wave (BOW) or a mixed $2k_F+4k_F$ BOW, which is why we termed it a "bond-charge-density wave" (BCDW).[17–19] In the present paper, we examine critically the theoretical and experimental evidence for each of these two possible charge orderings in the quasi-1D organic CTS. Before proceeding to our analysis, it is useful to formulate in a precise manner several key questions related to the charge ordering in the organic CTS. We focus here on four such questions.

First, the $\ldots 1010 \ldots$ CO ground state requires both strong on-site Coulomb repulsion ($U \gg t_0$ within the extended Hubbard model) *and* nearest-neighbor Coulomb repulsion (V within the extended Hubbard model) to be greater than a critical value, $V_c(U)$. For any comparison to real materials determining the correct value $V_c(U)$ is essential. Both Hartree-Fock (HF) and exact many-body methods have been used to estimate $V_c(U)$. How reliable are the HF estimates quantitatively, and do they exhibit the correct qualitative trends as U varies?

Second, charge ordering is only one of the phenomena observed in organic CTS. At lower temperatures, broken symmetry states involving spin ordering—spin-Peierls (SP) and spin-density wave (SDW) states—are typically observed, to say nothing of superconductivity. Many of the quasi-1D CTS materials that show CO also feature SP ground states at low temperature. Our previous work[17–19] establishing the BCDW state proves that the 1100 CO *is* consistent with SP. To our knowledge, none of the theoretical studies proposing the existence of $\ldots 1010 \ldots$ CO[20,26] has investigated whether a SP phase can occur within the $\ldots 1010 \ldots$ CDW at lower temperatures. Indeed, an early quantum Monte Carlo study[27] can be taken to suggest that a SP phase could *not* coexist with the $\ldots 1010 \ldots$ CDW. Is 1010 CO consistent with a SP phase at low temperatures, and if so, under what conditions?

Third, any successful theory of charge ordering within the organic CTS must explain not only the mechanism and pattern for CO, but also the temperature scale at which it occurs. In particular, any complete theory of CO in these materials must be able to explain the existence of different temperatures for the metal-insulator (MI), CO, and SP transitions.

Does either of the theoretical models for CO explain the observed sequence of transitions?

Fourth, the ultimate arbiter in the $\ldots 1010 \ldots$ vs $\ldots 1100 \ldots$ debate is experiment, and in this regard it is clearly desirable to have as broad a range of probes and materials as possible. Both the 2:1 cationic CTS (with holes as carriers) and the 1:2 anionic CTS (with electrons as carriers) have been studied extensively using similar theoretical and experimental approaches. What is the experimental evidence for $\ldots 1010 \ldots$ and for $\ldots 1100 \ldots$ in both these classes of materials?

We address these questions in the remainder of this paper. In Sec. II we introduce the the electronic extended Hubbard model and compare exact to mean-field calculations. Here we establish that the HF theory exaggerates the role of the $\ldots 1010 \ldots$ CO and that the *realistic* range of parameter values for which this CO is obtained is rather narrow. In Sec. III we introduce *e-ph* couplings and show that it *is* possible for a spin-Peierls transition to occur with the $\ldots 1010 \ldots$ CO phase. In Sec. IV, we discuss the theoretical expectations for the sequence of temperatures at which the various transitions–MI, CO, and SP—occur, establishing that within the strictly 1D $\ldots 1100 \ldots$ CO model, $T_{MI} > T_{CO} = T_{SP}$, whereas within the strictly 1D $\ldots 1010 \ldots$ CO model, $T_{MI} = T_{CO} > T_{SP}$. In Sec. V we compare our theoretical results with experimental data on a wide variety of CTS, both cationic and anionic. These comparisons establish that in both the anionic 1:2 CTS and the $(TMTSF)_2X$, the dominant CO pattern appears to be $\ldots 1100 \ldots$, which in the latter case coexists with a SDW (because of two-dimensional effects[19]) rather than a SP phase. For the $(TMTTF)_2X$ CTS, the situation appears less certain. We propose specific experiments to distinguish definitively between the two different CO patterns. Finally, in Sec. VI, we summarize our results and list some open problems for future research.

II. THE 1D EXTENDED HUBBARD HAMILTONIAN

We first consider the 1D extended Hubbard Hamiltonian

$$H = H_0 + H_{ee}, \tag{1a}$$

$$H_0 = -t_0 \sum_{j,\sigma} [c^{\dagger}_{j,\sigma} c_{j+1,\sigma} + c^{\dagger}_{j+1,\sigma} c_{j,\sigma}], \tag{1b}$$

$$H_{ee} = U \sum_j n_{j,\uparrow} n_{j,\downarrow} + V \sum_j n_j n_{j+1}. \tag{1c}$$

In the above, j is a site index, $n_j = n_{j,\uparrow} + n_{j,\downarrow}$, and σ is spin. We focus on the $\frac{1}{4}$-filled case, with the average number of electrons (or holes) per site, $\rho = \frac{1}{2}$. In addition to the purely electronic terms in Eq. (1), we will also consider *e-ph* couplings explicitly in Sec. III.

That for $U \to \infty$ there exists a critical value (V_c) of V for the appearance of the $4k_F$ CDW ($\ldots 1010 \ldots$) within the $\frac{1}{4}$-filled 1D ''pure'' extended Hubbard model in Eq. (1) has been known for decades,[28] and several detailed studies of V_c for finite U have appeared in recent years.[29–31] Nonetheless, it appears that the implications of these theoretical results have been insufficiently appreciated in the recent literature on organic CTS. Thus, we believe these results and the underlying arguments bear revisiting briefly here. In the limit $U \to \infty$, the $\frac{1}{4}$-filled band of spin-$\frac{1}{2}$ electrons becomes equivalent to a half-filled band of spinless fermions,[32,33] which in the presence of V can be mapped using a Jordan-Wigner transformation to the Heisenberg XXZ chain. This rigorous mapping and the exact solution for the XXZ model establish that for $V > 2t_0$, the system is in the (gapped) ''Ising-Heisenberg'' phase, which in terms of the original electronic model corresponds to the $4k_F$ CDW order $\ldots 1010 \ldots$ For $V < 2t_0$, the spin system is in the ''Heisenberg-XY'' phase and there is no gap, which in the *pure* extended Hubbard model corresponds to a Luttinger liquid with no charge order. Hence for $U \to \infty$, the critical value of V is $V_c(\infty) = 2t_0$.

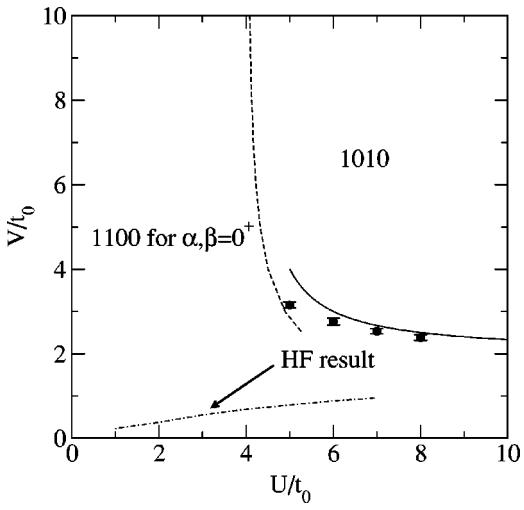

FIG. 1. Phase diagram of the 1D extended Hubbard model at quarter filling for positive values of U and V. The $4k_F$ CDW exists only in the upper right-hand corner, above the value of $V_c(U)$ determined by the two strong-coupling curves (solid line, $U \to \infty$; dashed line, $V \to \infty$) and the quantum Monte Carlo data points. Dashed-dotted line, Hartree-Fock data.

For finite U, the value of V_c has been calculated (i) within strong-coupling perturbation theory around $U \to \infty$, where a second-order calculation yields[30] $V_c(U) \simeq 2t + 2t^2/(U - 4t) + \cdots$; (ii) within strong-coupling theory in the limit $V \to \infty$, where a similar second-order calculation shows[29,30] that for finite V the $4k_F$ CDW phase boundary occurs at $U_c(V) \simeq 4t + (8t^3/V^2) + \cdots$; and (iii) for intermediate values of U and V by both exact diagonalization[29] and quantum Monte Carlo methods.[30,31] In Fig. 1 we show the resulting boundary of the $4k_F$ CDW phase in the U, V plane; in this figure, the solid and dashed curves represent the two strong-coupling expansions and the points with error bars represent our new determination of the boundary at intermediate coupling using a quantum Monte Carlo approach described in Ref. 31.

The relevance of presenting the true phase boundary in the U, V plane (as determined by accurate many-body methods) becomes clear when one considers the results obtained in a number of recent studies of the $\frac{1}{4}$-filled 1D extended

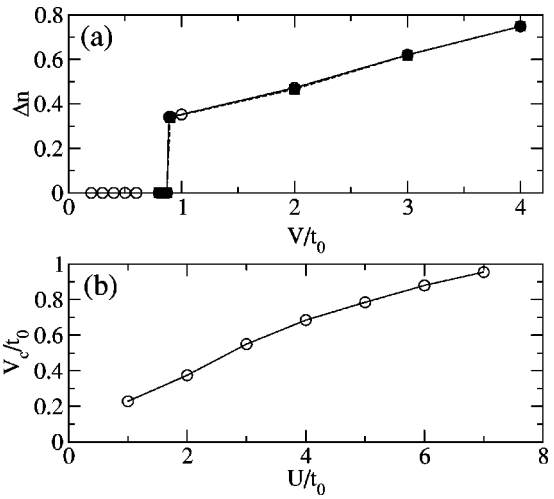

FIG. 2. (a) Charge disproportiation Δn vs V within the HF approximation for $U=6t_0$. Open (filled) symbols are for $N=16$ ($N=32$) rings. (b) V_c within the HF approximation. Lines are guides to the eye.

Hubbard model using mean-field approximations.[20,22,23] Using the HF approximation for the U interaction, and Hartree for the V interaction, as is done in Refs. 20, leads to drastically reduced values of V_c compared to the true results: for $U=5t_0$, the mean field $V_c^{MF}=0.4t_0$,[20] as compared to $V_c=(3.15\pm0.07)t_0$ expected from Fig. 1. In Fig. 2, we present results for our own unrestricted HF calculations on finite-size lattices. In these calculations, both U and V interactions were treated within the full HF approximation, and no assumptions are made about the periodicity of the solution. The value of V_c is readily determined by the point at which Δn, the difference between charge densities on adjacent sites, becomes nonzero [see Fig. 2(a)]. As seen in Fig. 2(a), finite-size effects are quite small, and V_c for the 64-site lattice did not differ significantly from 32 and 16 sites. From Fig. 2(b), we see that contrary to the known exact results for the 1D extended Hubbard model, *within the HF approximation* (i) the $\ldots 1010\ldots$ CDW does occur for $U<4t_0$, and (ii) the HF V_c *increases* with U. For direct comparison of exact and HF results, the data of Fig. 2(b) are plotted as the dashed-dotted line in Fig. 1 and clearly show that the mean-field approximations incorrectly increase the parameter regime in which $\ldots 1010\ldots$ CO is expected in the extended Hubbard model.

III. CHARGE AND SPIN ORDER INCLUDING PHONONS IN 1D

To answer the second question posed in the Introduction, we explore systematically the quantitative effects of adding *e-ph* interactions to the extended Hubbard model in Eq. (1), resulting in a ''Peierls-extended Hubbard'' (PEH) model. Our results establish that an SP transition *can* occur within the $\ldots 1010\ldots$ CO state and clarify the regions of *e-ph* parameter space, in which the two competing forms of charge order exist. Our PEH model follows from replacing the one-electron part H_0 in Eq. (1) by

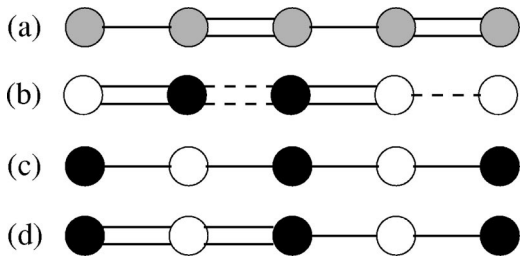

FIG. 3. The competing density wave ground states in the Peierls-extended Hubbard Model at $\frac{1}{4}$ filling. Gray, black, and white circles correspond to site charges of 0.5, $0.5+\epsilon$, and $0.5-\epsilon$, respectively. (a) The $4k_F$ BOW state, with dimerized bond orders $SWSW$ and uniform site charge densities. (b) The BCDW state, with bond orders $SW'SW$ and the accompanying CO $\ldots 1100\ldots$ (c) The $4k_F$ CDW with $\ldots 1010\ldots$ CO and uniform bond order. (d) The $4k_F$ CDW-SP state, with $\ldots 1010\ldots$ charge order and bond orders $SSWW$. The charges on the ''unoccupied'' sites in (d) are slightly different (see Fig. 5).

$$H_0=-\sum_{j,\sigma}[t_0-\alpha\Delta_j]B_{j,j+1,\sigma}+\beta\sum_j v_j n_j + \frac{K_1}{2}\sum_j \Delta_j^2+\frac{K_2}{2}\sum_j v_j^2. \quad (2)$$

In the above $\Delta_j=u_{j+1}-u_j$, where u_j is the displacement of the jth atom from equilibrium. The amplitude of the internal molecular vibration is given by v_j. α and β are the intersite and intrasite *e-ph* coupling constants, respectively, and K_1 and K_2 are the corresponding spring constants. The kinetic-energy operator $B_{j,j+1,\sigma}=c^\dagger_{j+1,\sigma}c_{j,\sigma}+c^\dagger_{j\sigma}c_{j+1,\sigma}$. We determine (numerically) self-consistent ground-state solutions for the above PEH model as functions of the parameters, measuring charge density $\langle n_j\rangle$ and bond order $\langle\Sigma_\sigma B_{j,j+1,\sigma}\rangle$.

We start with a summary of previous relevant results[17–19,24,25] concerning the SP transition in the $\frac{1}{4}$-filled band. These prior investigations have established that for $V<V_c$ and for nonzero α *or* β (or both), the dominant broken symmetry below the metal insulator, but above the insulator-insulator SP transition is the dimerized $4k_F$ BOW with uniform site charges [Fig. 3(a)]. The SP transition here is a *second* dimerization of the dimerized lattice, leading to the BCDW state, which can be considered as a superposition of the $2k_F$ and $4k_F$ BOW's, and which is accompanied by the $\ldots 1100\ldots$ CO [Fig. 3(b)]. The bond distortion pattern in the BCDW is $SW'SW$, where S is a strong bond, and W and W' are weaker bonds with $W'>W$. For $V>V_c$, the CO phase is the $\ldots 1010\ldots$ $4k_F$ CDW, which has uniform bond orders at high temperatures [Fig. 3(c)]. The SP phase within the $4k_F$ CDW phase, whose existence has not previously been studied or established, would correspond to Fig. 3(d). We demonstrate below the existence and nature of this phase, which we hereafter refer to as the $4k_F$ CDW-SP phase. Within the $4k_F$ CDW-SP phase, there occur alternate strong and weak bonds between the ''occupied'' sites that are actually second neighbors [see Fig. 3(d)], leading to a $SSWW$ bond-order pattern. Previous work did not find this $4k_F$ CDW-SP phase either because of focusing primarily on

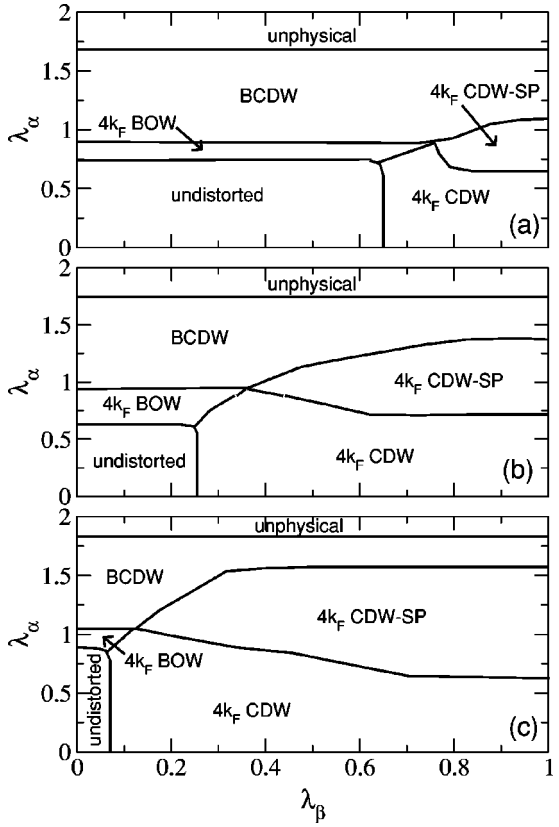

FIG. 4. The phase diagram in the $\lambda_\alpha - \lambda_\beta$ plane for $U=8t_0$ and (a) $V=2t_0$; (b) $V=3t_0$; and (c) $V=4t_0$ for a 16-site periodic ring. The boundaries between the the various phases, drawn as continuous lines in the figures, are actually determined numerically with an accuracy of ~ 0.05 in λ_α and λ_β. In the regions labeled ''unphysical,'' the weakest bonds have negative bond orders due to the excessive lattice distortion that occurs for very large λ_α.

$V<V_c$,[17–19] or because of including only one, but not *simultaneously both* of the *e-ph* couplings α and β.[24,25] In this section, we present new results for the $\frac{1}{4}$-filled band for both $V<V_c$ and $V>V_c$, including both *e-ph* couplings α and β.

We have performed fully self-consistent exact diagonalizations of finite-sized periodic rings. The self-consistency equations derived from $\partial\langle H\rangle/\partial\Delta_j=0$ and $\partial\langle H\rangle/\partial v_j=0$ are

$$\Delta_j=-\frac{\alpha}{K_1}\langle B_{j,j+1,\sigma}\rangle, \quad v_j=-\frac{\beta}{K_2}\langle n_j\rangle. \tag{3}$$

We present results in terms of dimensionless *e-ph* couplings $\lambda_\alpha=\alpha^2/(K_1 t_0)$ and $\lambda_\beta=\beta^2/(K_2 t_0)$. We have obtained results for systems of sizes $N=8$, 12, and 16. In Fig. 4 we present a ground-state phase diagram ($N=16$) in the $\lambda_\alpha - \lambda_\beta$ plane, showing regions, in which the various broken symmetry states dominate. In all cases, $U=8t_0$; panels (a), (b), and (c) correspond to $V=2t_0$, $3t_0$, and $4t_0$, respectively.

Consider Fig. 4(a) with $V=2t_0$. Since $U=8t_0$, this value of V lies below V_c for the infinite system (see Fig. 1). For this 16-site system, as we increase λ_α from zero (for fixed small λ_β), there is initially no distortion. For $\lambda_\alpha \gtrsim 0.7$, the ground state becomes the $4k_F$ BOW shown in Fig. 3(a); while the site charge densities remain uniform ($n=0.5$), the bond order is now inhomogeneous and has the form $SWSW$. For $\lambda_\alpha \gtrsim 0.9$, the BCDW discussed above and depicted in Fig. 3(b) becomes the ground state. Hence the bond-order pattern now is $SW'SW$ and the charge order has the $\ldots 1100 \ldots$ pattern. Next consider increasing λ_β from zero at fixed small λ_α. Again the state is initially undistorted, but when λ_β reaches a critical value, the $4k_F$ CDW with $\ldots 1010 \ldots$ charge order and uniform bond order becomes the ground state. Importantly, we see that a SP distortion *does* occur within the $\ldots 1010 \ldots$ charge-ordered region, but the resulting $4k_F$ CDW-SP state [shown in Fig. 3(d)] occurs only for fairly large values of both λ_α and λ_β when $U=8t_0$ and $V=2t_0$, at least for this 16-site system. Finally, we note that in the region labeled *unphysical* in Fig. 4 the value of λ_α has become so large that self-consistency drives the weakest hopping integral negative, rendering the results unphysical in this context.

Panels (b) and (c) of Fig. 4 show several important trends as V is increased through and beyond the value of $V_c(8t_0)$ for an infinite system. First, the sizes of the undistorted, $4k_F$ BOW and BCDW regions decrease considerably with increasing V and move to larger values of λ_α, showing that it takes stronger *e-ph* coupling to overcome the ''natural'' tendency toward $\ldots 1010 \ldots$ CO at large V. For the same reason, the sizes of the $4k_F$ CDW and $4k_F$ CDW-SP regions increase considerably with V and occur for smaller values of λ_β. Second, the existence of the $4k_F$ CDW-SP ground state is very robust—V does not appear to suppress this SP order. Third, Fig. 4 illustrates one clear qualitative difference between the two SP phases *in this finite-size system*. Provided that λ_α is greater than a critical value depending on V ($\lambda_{\alpha_c}(V)$), the BCDW occurs for all $\lambda_\beta \geqslant 0$. In contrast, the occurrence of the $4k_F$ CDW-SP state requires both λ_α and λ_β to be nonzero. Note, however, that as V is increased, the *minimum* value of λ_β [call it as $\lambda_{\beta_c}(V)$], for which the $4k_F$ CDW-SP state exists decreases rapidly towards zero, while the value of λ_α necessary to produce this phase at $\lambda_{\beta_c}(V)$ increases slightly.

These intriguing finite-size results beg the question of what happens to the system in the thermodynamic limit, $N \rightarrow \infty$. Unfortunately, our limited data do not allow us to perform a reliable finite-size scaling analysis, and we can thus provide only tentative, partial answers at this stage. We believe that in the $N \rightarrow \infty$ limit the undistorted and $4k_F$ BOW phases disappear; our evidence for this comes from our earlier studies of the BCDW (hence for $V<V_c$) on long *open* chains,[34] which showed that the center of these chains distorts naturally into a BCDW, but which showed no sign of a pure $4k_F$ BOW. Similar studies for $V>V_c$ have thus far proven inconclusive, and the $N \rightarrow \infty$ behavior in this regime remains an important open question.

Our self-consistent exact diagonalizations give results for site charges, bond orders, and hopping integrals for all the phases, homogeneous, and inhomogeneous. In Fig. 5 we present the actual site charge densities and bond orders for $U=8t_0$, $V=3t_0$, and $\lambda_\beta=0.6$. This plot corresponds to a

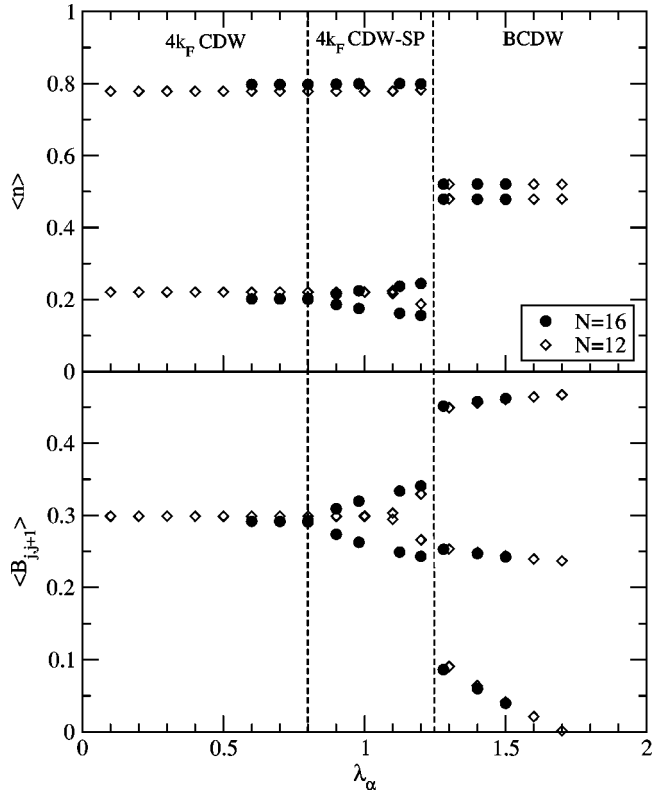

FIG. 5. Different possible values for charge densities and bond orders for $U=8t_0$, $V=3t_0$, and $\lambda_\beta=0.6$ (see Fig. 4(b)). Circles (diamonds) are data for $N=16$ ($N=12$) site rings.

vertical ''slice'' through Fig. 4(b), and shows the $4k_F$-CDW, $4k_F$-CDW-SP, and BCDW phases. Several points are suggested by the data in Fig. 5.

First, in the $4k_F$ CDW-SP state, the sites with smaller charge density are no longer equivalent—there is now (as expected from the bond distortion) a small charge difference between these two sites. Thus, the $4k_F$ CDW-SP state is characterized by two different bond orders and *three* different site charges, as opposed to the two different charges and three different bond orders of the BCDW state, which are also seen clearly in Fig. 5. We shall return to this point momentarily. Second, the quantitative values of the site charge differences Δn in the BCDW state are quite small, whereas the Δn in the $4k_F$ CDW, and $4k_F$ CDW-SP states are considerably larger. We have not been able to find, in our finite system calculations, any BCDW state with large Δn, nor any $4k_F$ CDW, or $4k_F$ CDW-SP states will be small Δn. Similarly, the bond-order differences in the BCDW are always quite large, whereas the bond-order differences in the $4k_F$ CDW-SP phase are always quite small. Again, these intriguing results for finite-size systems beg the question of the behavior for $N\rightarrow\infty$, and again we cannot provide definitive statements, because our data are not sufficient to allow a reliable finite-size scaling analysis. One argument suggesting that the large Δn may *not* be an inevitable consequence of the . . . 1010 . . . CO comes from the $U\rightarrow\infty$ limit and the mapping to the Heisenberg-Ising model; translating the exact results into fermion language shows that charge difference in the . . . 1010 . . . CO phase is given by $\Delta n\sim\exp-[1/(V-2t_0)]$, so that it starts from zero and remains small for a large region of $V>V_c=2t_0$.[28] Clearly, further study of these potentially significant differences in the $N\rightarrow\infty$ limit is required.

Beyond the quantitative distinctions, however, there is the clear *qualitative* distinction between the BCDW and the $4k_F$ CDW-SP states: namely, the former always has two different site charges and three different bond orders, whereas the latter has three different site charges and two different bond orders. This qualitative distinction will persist in the large system limit and is, in principle, accessible to experimental techniques sensitive to the local charge or bond-order environment. For instance, if NMR measurements can be made below the spin-Peierls transition temperature T_{SP} in a given CTS, they should be able to distinguish cleanly between the BCDW and the $4k_F$-CDW-SP states. We will return to this and related points in our comparisons to experiment.

IV. TEMPERATURE DEPENDENCE OF CO TRANSITIONS

Our calculations in Secs. III and II, as well as virtually all other theoretical studies, have been limited to ground-state results only. However, the issue of the temperature dependence of the CO and MI transitions is quite important in applying the results of 1D model calculations to experimental systems. In this section, we discuss the temperature dependence expected for . . . 1010 . . . and . . . 1100 . . . models of CO.

As the . . . 1010 . . . CO is driven by V, it is expected to give CO already at quite high temperatures. The series of transitions can be understood by recognizing that the . . . 1010 . . . CO has two equivalent configurations, . . . 1010 . . . and . . . 0101 . . . , corresponding to a double-well potential. For temperatures above the CO transition temperature, both possible configurations . . . 1010 . . . and . . . 0101 . . . have equal weight in the partition function, resulting in no net CO and a metallic state. The CO transition then corresponds to a symmetry breaking between . . . 1010 . . . and . . . 0101 . . . , with the result that CO and MI transitions (at T_{CO} and T_{MI}, respectively) happen at the *same* temperature. As we have shown in Sec. III, a SP distortion *can occur* within the . . . 1010 . . . CO phase, but its scale is set by the *e-ph* couplings and is expected to be well below the electronically driven $T_{MI}=T_{CO}$. Thus within the . . . 1010 . . . model [see Fig. 6(a)], one expects two transitions, a combined high-temperature CO/MI transition followed by a low-temperature SP transition.

In the . . . 1100 . . . CO model, one must consider a quadruple-well potential.[19] At the highest temperatures there are four equivalent configurations, . . . 1100 . . . , . . . 0011 . . . , . . . 0110 . . . , and . . . 1001 . . . , again giving a metallic state when all four have equal weights. The high-temperature transition corresponds to a symmetry breaking that leaves . . . 1100 . . . and . . . 0011 . . . with equal weight, resulting in no net CO, but an insulating state. Then at lower temperature, the . . . 1100 . . . / . . . 0011 . . . symmetry breaks, resulting in CO. As the . . . 1100 . . . CO

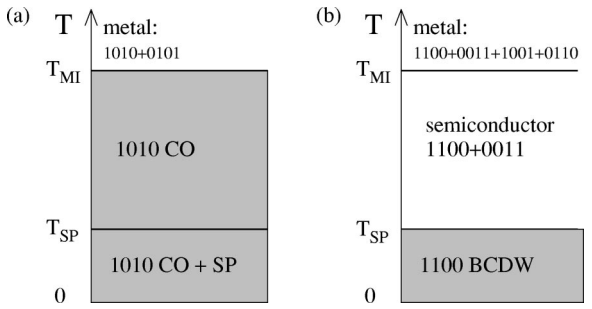

FIG. 6. Schematic showing expected temperature dependence of (a) $\ldots 1010 \ldots$ and (b) $\ldots 1100 \ldots$ CO models. T_{SP} and T_{MI} indicate SP and MI transition temperatures, respectively. The shaded region indicates temperature range where CO is found.

is a *cooperative* BCDW state, CO and bond distortion occurs *simultaneously*.[19] Thus within the $\ldots 1100 \ldots$ model [see Fig. 6(b)], one again expects two transitions, a high-temperature MI transition, followed by a low-temperature combined CO/SP transition.

V. INTERPRETATION OF EXPERIMENTS

If detailed comparisons of models to real systems are to be attempted, accurate estimates of the *e-e* and *e-ph* parameters are required. Determination of U and V from quantum chemistry calculations is difficult, and in general such calculations give values that are too large.[35] Fortunately, there is by now general agreement on the magnitudes of t_0 in the different materials, and reasonable values of U and V can be estimated from the experiments. We consider primarily materials based on the TCNQ, TMTSF, and TMTTF molecules. It is generally accepted that the values of t_0 in the cationic TMTTF/TMTSF and anionic TCNQ CTS lie between 0.1–0.25 eV. We then agree with previous investigators that U/t_0 in $(\mathrm{TMTTF})_2X$ ranges from 7–12,[35,36] and is less than 6 in $(\mathrm{TMTSF})_2X$.[36,37] Based on comparing relative $4k_F$ responses[38–40] (a signature of large U/t_0), one may conclude that for TCNQ systems U/t_0 is intermediate between the TMTTF and TMTSF limits. There are far fewer estimates of V/t_0: values of 2.8 for $(\mathrm{TMTTF})_2X$ and 2.0 for $(\mathrm{TMTSF})_2X$ have been proposed by Mila.[36] We note that whether or not $V>V_c(U)$ can be determined from the experimental pattern of the CO, if it is known. On the other hand, given the relatively small U/t_0 in $(\mathrm{TMTSF})_2X$, it is unlikely that $V>V_c(U)$ in this system (recalling the additional condition that $V<U/2$, based on general considerations of the nature of realistic Coulomb interactions.). To summarize, in the quasi-1D materials, we believe that $(U/t_0)^{TMTTF}>(U/t_0)^{TCNQ}>(U/t_0)^{TMTSF}$. For the *e-ph* couplings, the dimensionless coupling constants α^2/K_1t_0 and β/K_2t_0 are even more difficult to estimate.[41–43] For our overall purposes, it suffices to note that there is an evidence for both nonzero α and β. Finally, although in this paper we do not explicitly model the effects of transverse coupling of the 1D chains (see Ref. 19 for a quantitative discussion of these effects), we shall comment on these higher-dimensional effects in some of the experimental discussion below. In this regard, it is important to recall that the electronic anisotropy and effective *e-e* interaction strengths can vary *independently* among the CTS. The relative strength of the *e-e* interactions is measured by the ratios U/t_0 and V/t_0, whereas the effective dimensionality is measured by $t_\perp/t_0$. These three ratios vary considerably among the materials. In particular, the TMTTF materials are both highly 1D and very strongly correlated, whereas the TMTSF materials are less 1D and also less strongly correlated.

Let us turn now to discuss the experimental situations with individual classes of materials.

A. 1:2 anionic CTS

As mentioned in the Introduction, a complete understanding of the CO phenomenon in the $\frac{1}{4}$-filled band CTS requires that both cationic and anionic CTS be examined on the same footing. The anionic CTS are much older, and many different contradictory claims exist in the literature. We therefore focus only on the materials $\mathrm{MEM(TCNQ)_2}$, $\mathrm{TEA(TCNQ)_2}$, $\mathrm{(DMe\text{-}DCNQI)_2Ag}$, and $\mathrm{(DI\text{-}DCNQI)_2Ag}$ for which clear evidence for CO has been found.

The most direct evidence for the $\ldots 1100 \ldots$ CO has been found in $\mathrm{MEM(TCNQ)_2}$ and $\mathrm{TEA(TCNQ)_2}$. Careful neutron diffraction study of deuterated $\mathrm{MEM(TCNQ)_2}$ below T_{SP} has clearly established the $SW'SW$ bond distortion pattern associated with the $\ldots 1100 \ldots$ BCDW.[44] Similarly, x-ray[45–48] and neutron[49] measurements have established both the $SW'SW$ bond distortion and the $\ldots 1100 \ldots$ CO in $\mathrm{TEA(TCNQ)_2}$ at low temperatures.

The $\mathrm{(DI\text{-}DCNQI)_2Ag}$ system was originally claimed to show the $\ldots 1010 \ldots$ CO from NMR experiments.[5] It was pointed out by the present authors that some of the experimental results perhaps indicated the $\ldots 1100 \ldots$ order.[6] X-ray measurements on the structurally related $\mathrm{(DMe\text{-}DCNQI)_2Ag}$ found[50] both $4k_F$ and $2k_F$ reflections and also clearly indicated the $4k_F$ phase to be a BOW. This would again indicate the $\ldots 1100 \ldots$ CO to be in the $2k_F$ phase.[50] The results of the same measurements were less clear with $\mathrm{(DI\text{-}DCNQI)_2Ag}$ and it was suggested that while the $4k_F$ order in $\mathrm{(DMe\text{-}DCNQI)_2Ag}$ was a BOW, it was a CDW in $\mathrm{(DI\text{-}DCNQI)_2Ag}$.[50] The occurrence of different kinds of orders in these structurally related materials, though not impossible, would have been rather mysterious. This problem has been recently resolved by Menghetti and collaborators:[51] from detailed analysis of temperature-dependent vibronic and vibrational infrared absorptions in $\mathrm{(DI\text{-}DCNQI)_2Ag}$ these authors have shown that the low-temperature phase in this material is a $2k_F$ bond tetramerized phase with the $\ldots 1100 \ldots$ CO pattern.

To conclude, the CO in all 1:2 anionic CTS for which detailed experimental data are available shows the $\ldots 1100 \ldots$ pattern.

B. $(\mathrm{TMTSF})_2X$

There is a strong evidence for the $\ldots 1100 \ldots$ CO in this class of materials, as we now discuss. First, we have pointed out in the above that U/t_0 and V/t_0 in TMTSF are

very likely smaller than that in the TCNQ solids. Given the clear evidence for the . . . 1100 . . . CO in the 1:2 TCNQ solids, the occurrence of the . . . 1010 . . . CO in TMTSF therefore appears questionable. Specifically, previous parametrizations of $(TMTSF)_2X$ have all put $U/t_0 \leqslant 6$, which makes $V_c/t_0 \sim 2.8$. Taken together with the condition $V < U/2$, this makes the . . . 1010 . . . . order very unlikely.

Direct evidence for the . . . 1100 . . . order in $(TMTSF)_2X$ comes from the determination that (a) there exists a coexisting CDW-SDW in these systems below T_{SDW}, and (b) the periodicities of these density waves are both $2k_F$.[2,3] Since the . . . 1010 . . . CO would give a $4k_F$ charge periodicity, this can then immediately be ruled out. The coexisting CDW-SDW has been demonstrated in our previous quasi-2D calculation within the Hamiltonian of Eq. (2),[18] where we demonstrated that for small but nonzero interchain coupling the proper description of the ground state is a bond-charge-spin-density wave (BCSDW), with the CO being . . . 1100 . . .

C. $(TMTTF)_2X$

Nad *et al.* have found evidence for CO in various $(TMTTF)_2X$ materials from dielectric permittivity studies.[12–15] Observation of ferroelectric behavior[15] suggests removal of all symmetry elements, and based upon this it has been suggested that the CO pattern here is of the . . . 1010 . . . type[15,52] and is accompanied by anion motion. Independent and direct verifications of CO in $X = PF_6$ and AsF_6 have come from NMR studies.[11] However, while the presence of some form of CO in $(TMTTF)_2X$ is undisputed, we believe there is not yet enough evidence to say definitively whether the pattern of CO is . . . 1010 . . . or . . . 1100 . . . Below we list the problems associated with both the . . . 1010 . . . and . . . 1100 . . . CO scenarios in the $(TMTTF)_2X$ and suggest a plausible resolution.

As discussed in Sec. IV, for the . . . 1010 . . . CO one expects that $T_{CO} = T_{MI}$, which would mean that the $(TMTTF)_2X$ CTS would be CO insulators at room temperature. However, for $X = PF_6$ and AsF_6, $T_{CO} \sim 65$ K and 100 K, respectively,[11] which are much lower than T_{MI}. Further, recent NMR experiments on $X = AsF_6$ under pressure also find that the CO is very sensitive to pressure and is suppressed for pressures greater than 0.15 GPa.[53] If the CO in $(TMTTF)_2X$ is of the . . . 1010 . . . pattern and hence driven by large V, one would expect that increased $t_\perp/t_0$ from the application of pressure would have little effect on the CO.

There exist similar problems with the . . . 1100 . . . . CO scenario also. To begin with, the . . . 1100 . . . CO within our theory should occur only at T_{SP}, but T_{CO} is much larger than T_{SP} in the $(TMTTF)_2X$. Similarly, NMR experiments lead to estimates of a lower limit of 0.5 for Δn,[53] which is much larger than the Δn we find in our finite-size calculations within the . . . 1100 . . . phase.

A possible resolution to the above is that the higher-temperature CO found in $(TMTTF)_2X$ is indeed . . . 1010 . . . , while the lower-temperature SP state has . . . 1100 . . . CO. Transitions at finite temperature are determined not by the ground-state energy but by the free energy. At temperatures $T \leqslant T_{MI}$, the excitations of a strongly correlated system are predominantly spin excitations. Because of the greater multiplicities of high-spin states, the free energy at high T (but below T_{MI}) is then dominated by high-spin states. Consider now the fully ferromagnetic state, which is clearly described within the *spinless* fermion Hamiltonian limit of Eq. (1). Thus V_c in this state remains $2t_0$ even for finite U and is smaller than the V_c for the ground state with total spin $S=0$. For similar reasons we expect for finite U, V_c to increase progressively as the total spin S decreases. Therefore, for a system in which V is slightly lower than V_c $(S=0)$ but higher than V_c $(S=S_{max})$ we see that at high temperatures, where high-spin excitations are thermally accessible, the CO pattern can be . . . 1010 . . . At lower temperatures where the high-spin states become thermally inaccessible and the free energy is dominated by low-spin states there can be a switching to the . . . 1100 . . . CO. We are currently exploring this scenario in detail.

Finally, we suggest two experiments that can settle the issue of CO in $(TMTTF)_2X$. First, x-ray or neutron diffraction experiments can probe the actual bond distortions below the SP transition: with sufficient sensitivity, they should be able to distinguish the $SW'SW$ distortions associated with the . . . 1100 . . . CO from the $SSWW$ distortions associated with the . . . 1010 . . . CO. Second, as shown in Sec. III, we predict three different charges below T_{SP} for the case of the . . . 1010 . . . CO (rather than the two charges associated with the . . . 1100 . . . state). If NMR experiments can be extended to this temperature region, further splitting of the NMR lines is predicted. Unfortunately, our results also suggest that the charge difference between the two ''0''s is rather small, and an extremely sensitive probe might be necessary to determine the new splitting.

VI. CONCLUSION

Our conclusions can be summarized as follows. First, formation of the Wigner crystallike . . . 1010 . . . CO requires V within the 1D extended Hubbard model that is much larger than that predicted within mean-field theory. Further, mean-field theory predicts the incorrect behavior of $V_c(U)$ as a function of U. Accurate many-body calculations show that for finite U, $V_c(U) > 2|t_0|$ and increases with decreasing U.

Second, we have given a complete theory of the SP transition that can occur in the correlated 1D $\frac{1}{4}$-filled band. The SP phase with the . . . 1100 . . . CO is a BCDW, with two different charges and three different bonds, the bond distortion pattern being $SW'SW$. In contrast, the SP phase in the . . . 1010 . . . CO has two kinds of bonds and three distinct charges; the bond distortion pattern here is $SSWW$, and this distortion makes the charges on the sites labeled ''0'' unequal. Several distinct types of experiments have confirmed the existence of two kinds of charges and three kinds of bonds in a number of 1:2 anionic CTS. In $(TMTSF)_2X$, experiments find coexisting CDW and SDW with the *same* periodicity, which as discussed above precludes the . . . 1010 . . . CO. The situation in the $(TMTTF)_2X$ is less clear, as experiments showing the existence of CO do not directly measure the specific CO pattern. We know of no

experiments to date that have confirmed the existence of the three types of charges and two types of bonds associated with the SP phase of the $\ldots 1010 \ldots$. We believe that the NMR and x-ray experiments that could confirm this should have high priority.

Third, within the strictly 1D models, the two charge orders predict different scenarios for the temperature dependence of the CO. For the $\ldots 1100 \ldots$ CO, $T_{MI} > T_{CO} = T_{SP}$, whereas for the $\ldots 1010 \ldots$ CO, $T_{MI} = T_{CO} > T_{SP}$. Neither of these results is in agreement with all the experiments, which in general show $T_{MI} > T_{CO} > T_{SP}$. We believe that weakly 2D interchain couplings, which explain the transition from CDW-SP to CDW-SDW ground states in some of the materials,[19] may also be the key to understand the ordering of T_{MI}, T_{CO}, and T_{SP} in the different CTS. Support for this belief comes from recent results on the strongly 2D θ-(BEDT-TTF)$_2X$ materials, in which T_{MI} occurs simultaneously with T_{CO}, followed by a lower-temperature spin-gap transition.[54,55] This sequence of transition temperatures, as well as the 2D CO and spin-gap formation, can be understood within a 2D, sixfold coordinated lattice model with dominant $\ldots 1100 \ldots$ CO order.[56]

Fourth, our calculations suggest several problems for further study. Apart from the experiments seeking to confirm a "three-charge, two bond" $4k_F$-CDW-SP state, these include theoretical studies providing a full explanation of the sequence of MI, CO, and SP transitions as the temperature is decreased, an accurate determination of the phase diagram in the e-ph coupling constant plane in the thermodynamic limit, and a quantitative understanding of the role of broken symmetries associated with higher-spin states at finite temperature. We are currently investigating these theoretical issues.

Finally, during preparation of this paper we became aware of the recent work of Shibata *et al.*,[57] who investigated the purely electronic extended Hubbard model in 1D. Although they did not discuss the $\ldots 1100 \ldots$ charge ordering, their results for V_c are completely consistent with ours in Sec. II. They have also shown that dimerization increases V_c.

ACKNOWLEDGMENTS

S.M. acknowledges support from the NSF under Grant No. NSF-DMR-0101659. D.K.C. acknowledges support from the NSF under Grant No. NSF-DMR-97-12765. Numerical calculations were done in part at the NCSA. We thank F. Zamborszky, S. Brown, and M. Meneghetti for useful discussions.

*Current address: Department of Physics and Astronomy, Mississippi State University, Box 5167, Mississippi State, MS 39762.

[1] T. Sasaki and N. Toyota, Synth. Met. **70**, 849 (1995).
[2] J.P. Pouget and S. Ravy, J. Phys. I **6**, 1501 (1996).
[3] J.P. Pouget and S. Ravy, Synth. Met. **85**, 1523 (1997).
[4] S. Kagoshima *et al.*, Solid State Commun. **110**, 479 (1999).
[5] K. Hiraki and K. Kanoda, Phys. Rev. Lett. **80**, 4737 (1998).
[6] S. Mazumdar, S. Ramasesha, R.T. Clay, and D.K. Campbell, Phys. Rev. Lett. **82**, 2411 (1999).
[7] K. Hiraki and K. Kanoda, Phys. Rev. Lett. **82**, 2412 (1999).
[8] M. Meneghetti, C. Pecile, K. Kanoda, K. Hiraki, and K. Yakushi, Synth. Met. **120**, 1091 (2001).
[9] K. Miyagawa, A. Kawamoto, and K. Kanoda, Phys. Rev. B **56**, R8487 (1997).
[10] N. Biskup, J. Perenboom, J.S. Brooks, and J.S. Qualls, Solid State Commun. **107**, 503 (1998).
[11] D. Chow *et al.*, Phys. Rev. Lett. **85**, 1698 (2000).
[12] F. Nad, P. Monceau, and J. Fabre, J. Phys. IV **9**, Pr10 (1999).
[13] F. Nad, P. Monceau, C. Carcel, and J.M. Fabre, J. Phys.: Condens. Matter **12**, L435 (2000).
[14] F. Nad, P. Monceau, C. Carcel, and J.M. Fabre, Phys. Rev. B **62**, 1753 (2000).
[15] P. Monceau, F.Y. Nad, and S. Brazovskii, Phys. Rev. Lett. **86**, 4080 (2001).
[16] K. Miyagawa, A. Kawamoto, and K. Kanoda, Phys. Rev. B **62**, R7679 (2000).
[17] K.C. Ung, S. Mazumdar, and D. Toussaint, Phys. Rev. Lett. **73**, 2603 (1994).
[18] S. Mazumdar, S. Ramasesha, R.T. Clay, and D.K. Campbell, Phys. Rev. Lett. **82**, 1522 (1999).
[19] S. Mazumdar, R.T. Clay, and D.K. Campbell, Phys. Rev. B **62**, 13 400 (2000).
[20] H. Seo and H. Fukuyama, J. Phys. Soc. Jpn. **66**, 1249 (1997).
[21] H. Seo, J. Phys. Soc. Jpn. **69**, 805 (2000).
[22] N. Kobayashi and M. Ogata, J. Phys. Soc. Jpn. **66**, 3356 (1997).
[23] N. Kobayashi, M. Ogata, and K. Yonemitsu, J. Phys. Soc. Jpn. **67**, 1098 (1998).
[24] J. Riera and D. Poilblanc, Phys. Rev. B **59**, 2667 (1999).
[25] J. Riera and D. Poilblanc, Phys. Rev. B **62**, R16 243 (2000).
[26] R.H. McKenzie, J. Merino, J.B. Marston, and O.P. Sushkov, Phys. Rev. B **64**, 085109 (2001).
[27] J.E. Hirsch and D.J. Scalapino, Phys. Rev. B **29**, 5554 (1984).
[28] J.D. Johnson and B. McCoy, Phys. Rev. A **6**, 1613 (1972), and references therein.
[29] K. Penc and F. Mila, Phys. Rev. B **49**, 9670 (1994).
[30] H.Q. Lin, E.R. Gagliano, D.K. Campbell, E.H. Fradkin, and J.E. Gubernatis, in *The Physics and Mathematical Physics of the Hubbard Model*, NATO ASI Series B, Vol. 343, edited by D. Baeriswyl, D.K. Campbell, J.M.P. Carmello, F. Guinea, and E. Louis (Plenum, New York, 1995).
[31] R.T. Clay, A.W. Sandvik, and D.K. Campbell, Phys. Rev. B **59**, 4665 (1999).
[32] D.J. Klein and W.A. Seitz, Phys. Rev. B **10**, 3217 (1974).
[33] J. Bernasconi, M.J. Rice, W.R. Schneider, and S. Strassler, Phys. Rev. B **12**, 1090 (1975).
[34] R.T. Clay, S. Mazumdar, and D.K. Campbell, Phys. Rev. Lett. **86**, 4084 (2001).
[35] F. Castet, A. Fritsch, and L. Ducasse, J. Phys. I **6**, 583 (1996).
[36] F. Mila, Phys. Rev. B **52**, 4788 (1995).
[37] C.S. Jacobsen, J. Phys. C **19**, 5643 (1986).
[38] S. Mazumdar and A.N. Bloch, Phys. Rev. Lett. **50**, 207 (1983).
[39] J.P. Pouget, Semicond. Semimetals **27**, 87 (1988).
[40] S. Kagoshima, J.P. Pouget, and H. Anzai, J. Phys. Soc. Jpn. **52**, 1629 (1983).
[41] D. Pedron, R. Bozio, M. Meneghetti, and C. Pecile, Phys. Rev. B **49**, 10 893 (1994).

[42] D. Pedron, A. Speghini, V. Mulloni, and R. Bozio, J. Chem. Phys. **103**, 2795 (1995).
[43] M. Meneghetti, A. Toffoletti, and L. Pasimeni, Phys. Rev. B **54**, 16 353 (1996).
[44] R.J.J. Visser, S. Oostra, C. Vettier, and J. Voiron, Phys. Rev. B **28**, 2074 (1983).
[45] H. Kobayashi, Y. Ohashi, F. Marumo, and Y. Saito, Acta Crystallogr., Sect. B: Struct. Crystallogr. Cryst. Chem. **B26**, 459 (1970).
[46] A. Filhol and M. Thomas, Acta Crystallogr., Sect. B: Struct. Sci. **B40**, 44 (1984).
[47] J.P. Farges, J. Phys. (France) **46**, 465 (1985).
[48] J.P. Farges, J. Phys. (France) **46**, 1249 (1985).
[49] A. Filhol, C.M.E. Zeyer, P. Chenavas, and J. Gaultier, Acta Crystallogr., Sect. B: Struct. Crystallogr. Cryst. Chem. **B36**, 2719 (1980).
[50] Y. Nogami, K. Oshima, K. Hiraki, and K. Kanoda, J. Phys. I **9**, 357 (1999).
[51] M. Meneghetti, C. Pecile, K. Yakushi, K. Yamamoto, K. Kanoda, and K. Hiraki, J. Solid State Chem. **168**, 632 (2002).
[52] J. Riera and D. Poilblanc, Phys. Rev. B **63**, 241102 (2001).
[53] F. Zamborszky *et al.*, Phys. Rev. B **66**, 081103 (2002).
[54] H. Mori, S. Tanaka, T. Mori, A. Kobayashi, and H. Kobayashi, Bull. Chem. Soc. Jpn. **71**, 797 (1998).
[55] H. Mori, S. Tanaka, and T. Mori, Phys. Rev. B **57**, 12 023 (1998).
[56] R.T. Clay, S. Mazumdar, and D.K. Campbell, J. Phys. Soc. Jpn. **71**, 1816 (2002).
[57] Y. Shibata, S. Nishimoto, and Y. Ohta, Phys. Rev. B **64**, 235107 (2001).